Experimental Synthesis of Strained Monolayer Silver Arsenide on Ag(111) Substrates *

Shuai Zhang(张帅)[1,2], Yang Song(宋洋)[1,2], Hang Li(李航)[1,2], Jin-Mei Li(李金梅)[3], Kai Qian(钱凯)[1,2], Chen Liu(刘晨)[3], Jia-Ou Wang(王嘉鸥)[3], Tian Qian(钱天)[1], Yu-Yang Zhang(张余洋)[1,2,4], Jian-Chen Lu(卢建臣)[5], Hong Ding(丁洪)[1,2,4], Xiao Lin(林晓)[1,2,4**], Jinbo Pan(潘金波)[1,2**], Shi-Xuan Du(杜世萱)[1,2,4], Hong-Jun Gao(高鸿钧)[1,2,4**]

[1]*Institute of Physics, Chinese Academy of Sciences, Beijing 100190, China*
[2]*School of Physical Sciences, University of Chinese Academy of Sciences, Chinese Academy of Sciences, Beijing 100190, China*
[3]*Institute of High Energy Physics, Chinese Academy of Sciences, Beijing 100190, China*
[4]*CAS Center for Excellence in Topological Quantum Computation, University of Chinese Academy of Sciences, Beijing 100190, China*
[5]*Kunming University of Science and Technology, Kunming 650500, China*

(Received 18 April 2020)

Two-dimensional (2D) materials are playing more and more important roles in both basic sciences and industrial applications. For 2D materials, strain could tune the properties and enlarge applications. Since the growth of 2D materials on substrates is often accompanied by strain, the interaction between 2D materials and substrates is worthy of careful attention. Here we demonstrate the fabrication of strained monolayer silver arsenide (AgAs) on Ag(111) by molecular beam epitaxy, which shows one-dimensional stripe structures arising from uniaxial strain. The atomic geometric structure and electronic band structure are investigated by low energy electron diffraction, scanning tunneling microscopy, x-ray photoelectron spectroscopy, angle-resolved photoemission spectroscopy and first-principle calculations. Monolayer AgAs synthesized on Ag(111) provides a platform to study the physical properties of strained 2D materials.

PACS: 81.15.−z, 81.05.Zx, 82.20.Wt DOI: 10.1088/0256-307X/37/6/068103

The first two-dimensional (2D) material, graphene, previously predicted to be unstable,[1] has been prepared by mechanical exfoliation of graphite.[2,3] After that, 2D materials attract tremendous attention, and develop rapidly, forming several species: graphene family, 2D chalcogenides, 2D oxides and so on.[4−6] Two-dimensional materials can be fabricated by several methods, for instance, mechanical exfoliation, surface growth,[7] solution-phase growth, and vapor growth.[8,9] Lots of discoveries of intriguing physical properties of 2D materials have been made in optics,[10] mechanics,[11] thermology,[12] topology,[13] magnetics[14,15] and electronics.[16] Diverse properties further lead to enormous applications.[17−22] For example, solution-processed MoS_2 films with excellent mobilities and on/off ratios have been used in transistors.[23]

For 2D materials, strain could be of vital importance and modulate the physical properties dramatically. For instance, strain induced topological phase transition has been observed on ultrathin Bi(111) films grown on Bi_2Te_3(111) substrates.[24] Strain is often introduced due to the interaction between 2D materials and substrates, accompanied by the occurrence of moiré patterns.[25−27] Recently, honeycomb monolayer CuSe with one-dimensional (1D) moiré pattern has been fabricated, which exhibits the Dirac nodal line fermion, protected by mirror reflection symmetry.[28] Motivated by these investigations, we aim at constructing a new strained 2D material on a substrate.

Here we report the epitaxy synthesis of monolayer strained silver arsenide (AgAs) on Ag(111) surface. Combined with low energy electron diffraction (LEED), scanning tunneling microscopy (STM), x-ray photoelectron spectroscopy (XPS), angle-resolved photoemission spectroscopy (ARPES) and first principles calculations, we reveal the atomic structure and band structure of monolayer silver arsenide on Ag(111) surface. Interestingly, the strain in one direction is larger than that in the other two, which makes 1D stripes appear in the monolayer AgAs.

The sample was prepared by a commercial ultrahigh-vacuum (UHV) molecular beam epitaxy combined system with a base pressure of about 1×10^{-9} mbar. Ag(111) single crystal was sputtered by Ar^+ ions and annealed for several cycles to attain an atomic clean surface. The quality of surface was checked by STM and LEED. Pure arsenic atoms were evaporated on the heated Ag(111) substrate (200 ℃) in UHV, then the sample was annealed

*Supported by the National Key Research & Development Program of China (Grant Nos. 2016YFA0202300 and 2018YFA0305800), the National Natural Science Foundation of China (Grant Nos. 61888102, 11604373, 61622116, and 51872284), the Strategic Priority Research Program of Chinese Academy of Sciences (Grant Nos. XDB30000000 and XDB28000000), and the University of Chinese Academy of Sciences.
**Corresponding authors. Email: xlin@ucas.ac.cn; jbpan@iphy.ac.cn; hjgao@iphy.ac.cn

at about 200 ℃ for 1 hour, and finally slowly cooled down. The as-grown sample was characterized by STM and LEED. *Ex-situ* XPS and ARPES measurements are performed by transferring the samples by a UHV transfer suit without breaking the vacuum. STM and ARPES experiments were carried out under 10 K, while XPS and LEED were performed at room temperature. ARPES experiments used HeⅡ ($h\nu = 40.6$ eV) resonance lines and a VG SCIENTA R4000 analyzer with angular and energy resolution 0.2° and 30 meV, respectively. XPS measurements were performed at Beijing Synchrotron Radiation Facility, with energy resolution better than 100 meV.

Quantum mechanical calculations based on density functional theory (DFT) were performed using the projector augmented wave (PAW) method with the local density approximation (LDA) functional,[29] as implemented in the Vienna Ab initio Simulation Package (VASP) code.[30,31] The spin–orbit coupling (SOC) effect is considered. The wavefunctions are expanded in plane wave basis with a kinetic energy cutoff of 400 eV. A slab model consisting of the monolayer AgAs and three Ag layers is used to simulate the strained monolayer AgAs on Ag(111) surface (Fig. 3). The size of the supercell is 4.90 Å×36.80 Å. The vacuum layer is ∼ 20 Å. The AgAs monolayer and top layer of Ag atoms are fully relaxed until the residual forces on each atom are smaller than 0.05 eV/Å, while the Ag atoms in the two bottom layers are fixed. The k-point sampling is $39 \times 1 \times 1$. A slab model consisting of 1×1 monolayer AgAs on $\sqrt{3} \times \sqrt{3}$ ten-layered Ag(111) is used to investigate the electronic properties of AgAs monolayer on the silver substrate in Fig. 4. The size of the unit cell is 4.90 Å × 4.90 Å. All AgAs atoms and Ag atoms in the top two layers are fully relaxed until the residual forces on each atom are smaller than 0.01 eV/Å. The k-point sampling is $39 \times 39 \times 1$.

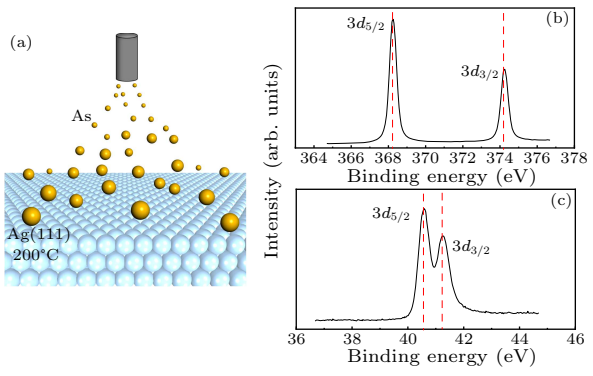

Fig. 1. The fabrication and XPS characterization of monolayer AgAs on the Ag(111) substrate. (a) Schematic of the molecular-beam-epitaxy growth process of AgAs. (b) XPS measurement from the core level of Ag features two peaks at 368.26 eV (Ag $3d_{5/2}$) and 374.28 eV (Ag $3d_{3/2}$). (c) XPS core-level spectra of As. Two prominent peaks are located at 40.58 eV (As $3d_{5/2}$) and 41.27 eV (As $3d_{3/2}$).

The growth schematic of the monolayer silver arsenide is shown in Fig. 1(a). Arsenic atoms are evaporated onto the elevated Ag(111) substrate, then the sample is annealed at 200 ℃. After growth of the sample, high-resolution XPS measurement is performed. Figures 1(b) and 1(c) show the XPS spectra from the core level of the Ag $3d$ and As $3d$, respectively. In Fig. 1(b), there are two significant peaks at 368.26 eV and 374.28 eV, which could be assigned to Ag $3d_{5/2}$ and $3d_{3/2}$, respectively. The positions of the two peaks agree well with elemental silver,[32] which is attributed to the fact that the quantity of elemental silver in the substrate is much greater than that in the silver arsenide monolayer. In contrast to Ag, the signal of As is not influenced by the substrate. In Fig. 1(c), the XPS spectra can be divided into two peaks locating at binding energy of 40.58 eV and 41.27 eV, which is the signal of As $3d_{5/2}$ and $3d_{3/2}$. According to the previous study,[33] the position of elemental As $3d_{5/2}$ is 41.62 eV. The XPS results reveal that the As atoms are bonded with Ag atoms.

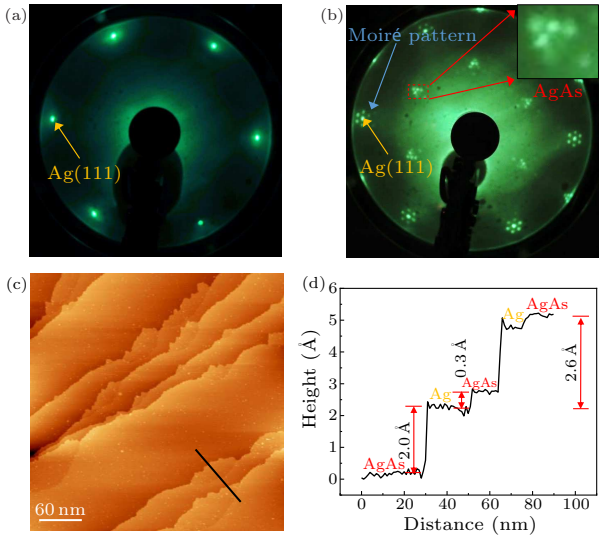

Fig. 2. LEED pattern and large-scale STM image of monolayer AgAs grown on the Ag(111) substrate. (a) LEED pattern of the Ag(111) substrate without arsenic. (b) LEED pattern of monolayer AgAs on Ag(111). Yellow, red, and blue arrows point out diffractive patterns of the Ag(111) substrate, monolayer AgAs, and moiré pattern, respectively. The inset shows the magnified image of the dotted rectangle. (c) Large-scale STM image of AgAs ($I = 0.05$ nA, $V = -1$ V). (d) Height profile along the black line in panel (c).

The structure of the AgAs monolayer is characterized by LEED at room temperature. Figure 2(a) shows a clear LEED pattern of the Ag(111) substrate before the deposition of arsenic, indicating that the surface is clean and ordered. After the deposition of arsenic and post-annealing, the new spots (marked by the red arrows) originating from AgAs monolayer appear at the positions of $(\sqrt{3}\times\sqrt{3})R30°$ with respect to Ag(111) spots, as shown in Fig. 2(b). These newly appeared spots are not single-dots, but composed of several little dots as shown in the inset of Fig. 2(b), which implies that monolayer AgAs has several series of lattices with similar but different lattice constants. It is

possible that anisotropically stressed lattices could result in these kinds of LEED patterns. The diffractive dots (indicated by the blue arrows) surrounding the Ag(111) patterns are most likely to originate from the moiré patterns, which is the result of the lattice mismatch of the substrate and the silver arsenide. Figure 2(c) is a typical large-scale STM image of the AgAs monolayer grown on Ag(111). The surface is uniform and there are no significant features except steps. As shown in Fig. 2(d), two kinds of steps are observed and the step heights are 2.0 Å nm and 0.3 Å. Here 2.0 Å is the vertical distance from AgAs on the lower step to Ag(111), while 0.3 Å is the height of AgAs relative to lateral Ag(111). As a result, the real height of AgAs is 2.6 Å relative to upper Ag(111), confirming the monolayer structure of the as-grown AgAs sample.

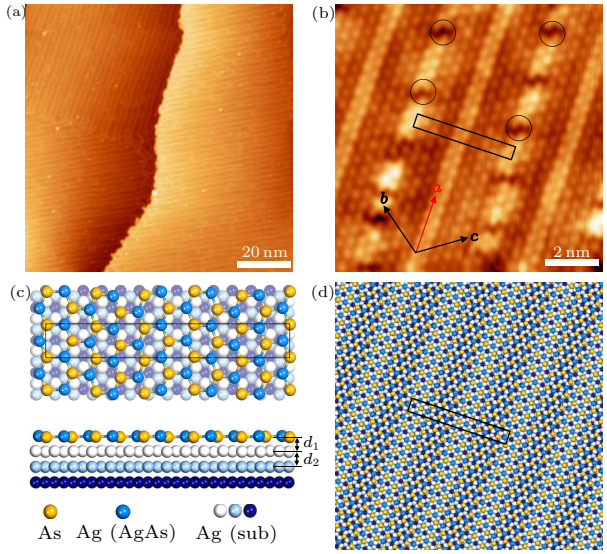

Fig. 3. Close-up STM images and atomic model of AgAs on Ag(111). (a) STM image presents a step edge and 1D stripes with different orientations ($I = 0.05$ nA, $V = -1$ V). (b) Atomic-resolved STM image. Here $\boldsymbol{a}$, $\boldsymbol{b}$ and $\boldsymbol{c}$ represent the three directions ($I = 5$ nA, $V = -10$ mV). (c) Top and side views of the optimized atomic structure model, showing a slightly distorted honeycomb structure. Yellow balls and blue balls denote As and Ag atoms, respectively. White, light blue and purple balls denote the Ag atoms of the Ag(111) substrate. (d) The optimized atomic structure model of AgAs on Ag(111) will reproduce the 1D stripes.

Figure 3(a) presents a zoom-in STM image of another sample with larger coverage, in which 1D stripes clearly appear. The stripes have three equivalent directions with angle of 120° between two directions, resulting in the hexagonal moiré patterns in Fig. 2(b). The atomic-resolved STM image (Fig. 3(b)) clearly shows the atomic structure of the AgAs. In addition, the lattice constant along the direction of the stripe (red line, 4.89±0.2 Å) is slightly larger than that along the other two directions (two black lines, 4.70 ± 0.2 Å and 4.68 ± 0.2 Å). Besides the 1D stripes, another feature presented in the STM image is the defect-like structures (indicated by the black circle in Fig. 3(b)). Because of the limited resolution of the STM instrument, we cannot give an exact model of the defect-like structure, but it may be related to atoms missing for releasing the strain.[34] Based on the STM and LEED results, combined with DFT calculations, we propose an atomic model of the AgAs layer as shown in Fig. 3(c). The model starts with a honeycomb structure with arsenic atoms and silver atoms alternately arranged, giving a structure close to $(\sqrt{3} \times \sqrt{3})R30°$ superstructure with respect to Ag(111) surface, which is in agreement with the LEED results. Because of the lattice mismatch between calculated freestanding AgAs monolayer and the substrate, the DFT optimized AgAs/Ag(111) model reveals the existence of uniaxial tension in AgAs monolayer on the Ag substrate. AgAs lattice is extended in one direction (direction a in Fig. 2(b)) to perfectly match the Ag substrate but not in other directions, which results in a one-dimensional moiré pattern, i.e., the 1D stripe in STM images. From the side view in Fig. 3(c), the height of AgAs relative to Ag(111) is similar to that of step height of Ag(111). However, in the STM image of Fig. 2(c), the apparent height of AgAs is slightly higher than the step height of Ag(111) in Fig. 2(d), due to strong couplings with electronic states of the sample in the STM imaging process. As shown in Fig. 3(d), the optimized structure model of AgAs on Ag(111) surface mimics the 1D stripe perfectly, in good agreement with the STM image (Fig. 2(b)). It should be mentioned that silver atoms are difficult to resolve in STM images,[35] due to their smaller density of state relative to arsenic atoms, and the bright little dots in the atomic-resolved STM image are from arsenic atoms. In short, we demonstrate that we have grown strained monolayer silver arsenide on Ag(111).

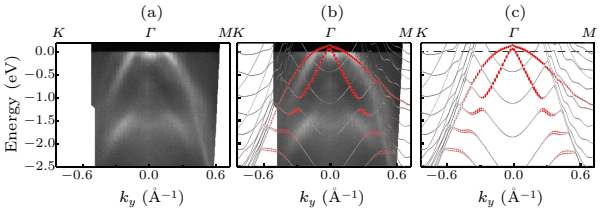

Fig. 4. Electronic band structure of AgAs monolayer. (a) ARPES intensity plots along K–Γ–M direction, including the bands of AgAs monolayer and the bands of the Ag(111) substrate. (b) ARPES measurements overlaid by calculation results with a small shift. Calculation results reproduce most bands, in agreement with the experimental data. (c) Calculated band structure of monolayer AgAs on Ag(111) including the SOC effect.

In order to investigate the electronic band structure of strained silver arsenide, ARPES measurements are carried out. Figure 4(a) shows the ARPES band dispersion along K–Γ–M direction of Brillouin zone of AgAs. Near the Fermi level, there are two hole-like bands. The electronic density of state at −1.5 eV arises from the silver substrate. DFT calculations with spin-orbit coupling (SOC) are carried out to obtain the band structures of monolayer AgAs on Ag(111), which are shown in Fig. 4(c). Calculated

results reproduce the hole-like bands, except those bands located at 0.2 eV. We think that the interaction between the silver arsenide and the silver substrate is strong and the Fermi level of the silver arsenide may be lifted by electron doping from the Ag substrate. In Fig. 4(b), we adjusted the Fermi surface of the calculated band structure to fit experiments and overlaid it on the ARPES intensity plot. The calculated results reproduce most of the bands detected by ARPES.

In summary, we have successfully fabricated strained monolayer AgAs on Ag(111) by molecular beam epitaxy. Combination results of STM, LEED, XPS and DFT calculations confirm the formation of $(\sqrt{3} \times \sqrt{3})R30^\circ$ superstructure of AgAs on Ag(111) surface. In addition, STM images and DFT calculations demonstrate the strain-induced 1D stripes originate from interaction of monolayer AgAs and the Ag substrate. ARPES and band calculation reveal the doped AgAs energy bands influenced by the Ag substrate. This work not only develops the method to synthesize a new 2D material, monolayer AgAs, but also offers a platform to investigate strain and interaction between 2D materials and substrates.

A portion of the research was performed in the CAS Key Laboratory of Vacuum Physics.

References

[1] Mermin N D 1968 *Phys. Rev.* **176** 250
[2] Novoselov K S, Geim A K, Morozov S V, Jiang D, Zhang Y, Dubonos S V, Grigorieva I V and Firsov A A 2004 *Science* **306** 666
[3] Novoselov K S, Geim A K, Morozov S V, Jiang D, Katsnelson M I, Grigorieva I V, Dubonos S V and Firsov A A 2005 *Nature* **438** 197
[4] Geim A K and Grigorieva I V 2013 *Nature* **499** 419
[5] Das S, Robinson J A, Dubey M, Terrones H and Terrones M 2015 *Annu. Rev. Mater. Res.* **45** 1
[6] Molle A, Goldberger J, Houssa M, Xu Y, Zhang S C and Akinwande D 2017 *Nat. Mater.* **16** 163
[7] Yu H L, Wu H Y, Zhu H J, Song G F and Xu Y 2017 *Chin. Phys. Lett.* **34** 018101
[8] Butler S Z, Hollen S M, Cao L, Cui Y, Gupta J A, Gutierrez H R, Heinz T F, Hong S S, Huang J, Ismach A F, Johnston-Halperin E, Kuno M, Plashnitsa V V, Robinson R D, Ruoff R S, Salahuddin S, Shan J, Shi L, Spencer M G, Terrones M, Windl W and Goldberger J E 2013 *ACS Nano* **7** 2898
[9] Wang J, Hu H Y, He Y R, Deng C, Wang Q, Duan X F, Huang Y Q and Ren X M 2015 *Chin. Phys. Lett.* **32** 088101
[10] Yu Y, Miao F, He J and Ni Z 2017 *Chin. Phys. B* **26** 036801
[11] Song Y, Mandelli D, Hod O, Urbakh M, Ma M and Zheng Q 2018 *Nat. Mater.* **17** 894
[12] Zhang G and Zhang Y W 2017 *Chin. Phys. B* **26** 034401
[13] Wang J, Niu J, Yan B, Li X, Bi R, Yao Y, Yu D and Wu X 2018 *Proc. Natl. Acad. Sci. USA* **115** 9145
[14] Pan L, Wen H, Huang L, Chen L, Deng H X, Xia J B and Wei Z 2019 *Chin. Phys. B* **28** 107504
[15] Han R and Yan Y 2018 *Chin. Phys. B* **27** 117505
[16] Mahmood J, Lee E K, Jung M, Shin D, Choi H J, Seo J M, Jung S M, Kim D, Li F, Lah M S, Park N, Shin H J, Oh J H and Baek J B 2016 *Proc. Natl. Acad. Sci. USA* **113** 7414
[17] Manzeli S, Ovchinnikov D, Pasquier D, Yazyev O V and Kis A 2017 *Nat. Rev. Mater.* **2** 17033
[18] Chhowalla M, Shin H S, Eda G, Li L J, Loh K P and Zhang H 2013 *Nat. Chem.* **5** 263
[19] Das S, Kim M, Lee J W and Choi W 2014 *Crit. Rev. Solid State Mater. Sci.* **39** 231
[20] Wang Q H, Kalantar-Zadeh K, Kis A, Coleman J N and Strano M S 2012 *Nat. Nanotechnol.* **7** 699
[21] Quhe R G, Wang Y Y and Lü J 2015 *Chin. Phys. B* **24** 088105
[22] Hisamuddin N, Zakaria U N, Zulkifli M Z, Latiff A A, Ahmad H and Harun S W 2016 *Chin. Phys. Lett.* **33** 074208
[23] Lin Z, Liu Y, Halim U, Ding M, Liu Y, Wang Y, Jia C, Chen P, Duan X, Wang C, Song F, Li M, Wan C, Huang Y and Duan X 2018 *Nature* **562** 254
[24] Hirahara T, Fukui N, Shirasawa T, Yamada M, Aitani M, Miyazaki H, Matsunami M, Kimura S, Takahashi T, Hasegawa S and Kobayashi K 2012 *Phys. Rev. Lett.* **109** 227401
[25] Liu Y, Rodrigues J N B, Luo Y Z, Li L, Carvalho A, Yang M, Laksono E, Lu J, Bao Y, Xu H, Tan S J R, Qiu Z, Sow C H, Feng Y P, Neto A H C, Adam S, Lu J and Loh K P 2018 *Nat. Nanotechnol.* **13** 828
[26] Yankowitz M, Xue J, Cormode D, Sanchez-Yamagishi J D, Watanabe K, Taniguchi T, Jarillo-Herrero P, Jacquod P and LeRoy B J 2012 *Nat. Phys.* **8** 382
[27] Guinea F, Katsnelson M I and Geim A K 2010 *Nat. Phys.* **6** 30
[28] Gao L, Sun J T, Lu J C, Li H, Qian K, Zhang S, Zhang Y Y, Qian T, Ding H, Lin X, Du S and Gao H J 2018 *Adv. Mater.* **30** 1707055
[29] Kohn W and Sham L J 1965 *Phys. Rev.* **140** A1133
[30] Kresse G and Furthmuller J 1996 *Comput. Mater. Sci.* **6** 15
[31] Kresse G and Furthmuller J 1996 *Phys. Rev. B* **54** 11169
[32] Anthony M T and Seah M P 1984 *Surf. Interface Anal.* **6** 95
[33] Powell C J 2012 *J. Electron Spectrosc. Relat. Phenom.* **185** 1
[34] Lin X, Lu J C, Shao Y, Zhang Y Y, Wu X, Pan J B, Gao L, Zhu S Y, Qian K, Zhang Y F, Bao D L, Li L F, Wang Y Q, Liu Z L, Sun J T, Lei T, Liu C, Wang J O, Ibrahim K, Leonard D N, Zhou W, Guo H M, Wang Y L, Du S X, Pantelides S T and Gao H J 2017 *Nat. Mater.* **16** 717
[35] Lu J, Bao D L, Qian K, Zhang S, Chen H, Lin X, Du S X and Gao H J 2017 *ACS Nano* **11** 1689